This article was downloaded by:
On: *25 January 2011*
Access details: *Access Details: Free Access*
Publisher *Taylor & Francis*
Informa Ltd Registered in England and Wales Registered Number: 1072954 Registered office: Mortimer House, 37-41 Mortimer Street, London W1T 3JH, UK

Separation Science and Technology

Publication details, including instructions for authors and subscription information:
http://www.informaworld.com/smpp/title~content=t713708471

Instability Mechanisms of Supported Liquid Membranes

T. M. Dreher; G. W. Stevens

To cite this Article Dreher, T. M. and Stevens, G. W.(1998) 'Instability Mechanisms of Supported Liquid Membranes', Separation Science and Technology, 33: 6, 835 — 853

To link to this Article: DOI: 10.1080/01496399808544879

URL: http://dx.doi.org/10.1080/01496399808544879

PLEASE SCROLL DOWN FOR ARTICLE

Full terms and conditions of use: http://www.informaworld.com/terms-and-conditions-of-access.pdf

This article may be used for research, teaching and private study purposes. Any substantial or systematic reproduction, re-distribution, re-selling, loan or sub-licensing, systematic supply or distribution in any form to anyone is expressly forbidden.

The publisher does not give any warranty express or implied or make any representation that the contents will be complete or accurate or up to date. The accuracy of any instructions, formulae and drug doses should be independently verified with primary sources. The publisher shall not be liable for any loss, actions, claims, proceedings, demand or costs or damages whatsoever or howsoever caused arising directly or indirectly in connection with or arising out of the use of this material.

SEPARATION SCIENCE AND TECHNOLOGY, 33(6), pp. 835–853, 1998

Instability Mechanisms of Supported Liquid Membranes

T. M. DREHER and G. W. STEVENS*
DEPARTMENT OF CHEMICAL ENGINEERING
THE UNIVERSITY OF MELBOURNE
PARKVILLE, VICTORIA 3052, AUSTRALIA

ABSTRACT

Supported liquid membranes (SLMs) have the ability to selectively separate low concentrations of metal and other ions from solution, and are therefore suited to waste treatment and process recycling operations. However, their application has been limited by their low flux and limited life. The extraction of copper across a supported liquid membrane using Acorga P5100 as the carrier was investigated. The effect of membrane liquid composition, and in particular its rheology on membrane stability and mass transfer, is discussed and modeled. Membrane instability mechanisms are discussed with reference to the proposed model and its effect in relation to the design of membrane units.

INTRODUCTION

Liquid membrane technology has been widely investigated due to its potential for a very selective, low cost, and energy-saving separation process. Traditional ion-exchange processes are able to separate, but often not selectively recover, metals from waste solutions. Therefore, liquid membrane separation techniques offer an attractive alternative to conventional solid or liquid ion-exchange processes. A reduction in the number of process steps, smaller quantity of expensive extractants required, and the ability of the process to extract all of the solute and produce a high concentration extract is economi-

---

* To whom correspondence should be addressed.

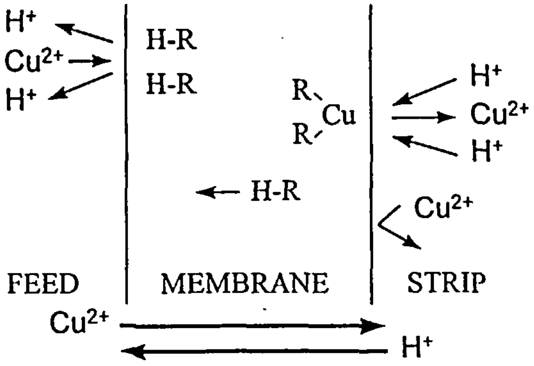

FIG. 1 Mechanism for transport through a supported liquid membrane.

cally attractive in many circumstances, especially where large volumes of solutions require treatment.

The transport of metal ions across supported liquid membranes (SLMs) is almost exclusively achieved via coupled transport where a carrier agent couples the flow of two or more species. For the case of copper extracted with Acorga P1 (Zeneca Pty. Ltd.), a hydrogen ion concentration gradient drives the transport of copper ions against their concentration gradient, thereby achieving uphill transport, as described by Danesi (1). The process is illustrated in Fig. 1.

Despite its many attractions, liquid membrane technology has not been widely implemented in industry due to concerns over membrane instability, which leads to a decrease in mass transfer, and eventually selectivity. Various mechanisms have been proposed for SLM instability, e.g., losses of the organic by dissolution, progressive wettability of the support pores, pressure differences across the membrane (1), and attrition of the organic film due to lateral shear forces (2, 3). However, no clear method of identifying which of the mechanisms is present has yet been proposed. Further research is required to understand the mechanisms of membrane liquid loss in SLMs before liquid membrane extraction processes suitable for industrial use may be developed. This paper presents an examination of these mechanisms for a flat-sheet membrane where copper is extracted with Acorga P5100.

EXPERIMENTAL TECHNIQUES

The experimental apparatus is shown schematically in Fig. 2. It consisted of two identical Perspex rectangular chambers, measuring 72 × 60 × 95

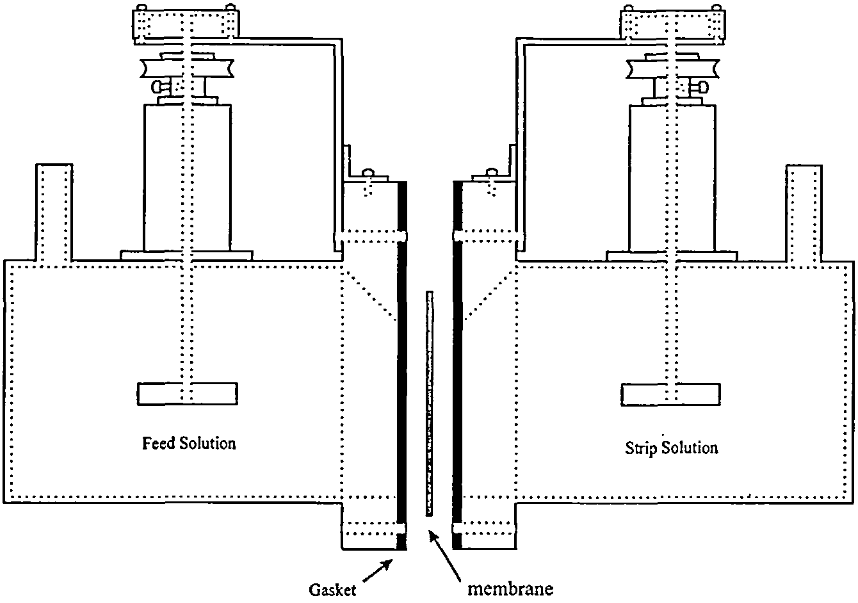

FIG. 2 Schematic of supported liquid membrane cell.

mm, with centrally located stainless steel impellers and Teflon bearings and bushing. Two sample ports on the top enabled filling and sampling of the solutions. A 60-mm^2 opening existed on one side face which was lined with a Norprene rubber gasket. The SLMs were prepared by pipetting the appropriate organic solution onto the polymeric support and holding it vertically to let the excess drain. The SLM was then placed between the two halves of the cell, which were screwed together to form a watertight seal. The impeller shafts were connected via a rubber O-ring to the same motor, set at 600 ± 5 rpm, so that their speeds were matched. The SLM cell was immersed in a circulating water bath held at 25 ± 0.1°C, leaving the tops of the sample ports and impeller shafts exposed. The strip solution was continuously monitored throughout each experiment, using a UV-Visible absorption spectrophotometer.

Reagents

The feed solution contained 24.57 g $CuSO_4 \cdot 5H_2O$ (98% pure, Merck) and approximately 0.02 g tartrazine (dye content 60%, Sigma-Aldrich) dissolved in distilled water ($\kappa < 10^{-6}$ S·cm^{-1}), giving a copper ion concentration of 9.44 × 10^{-2} M. The tartrazine was added as a nontransferring colored component that could be used to detect the breakdown of the membrane. The strip solution was made by diluting concentrated sulfuric acid (AR grade, Merck) with distilled water until the pH was measured to be 0.40.

Membranes

Experiments were performed using a GORE-TEX laminate (part number X19181, W. L. Gore & Associates Aust. Pty. Ltd.), which consisted of a hydrophobic PTFE membrane, pore size 0.45 μm, bonded to a nonwoven backing consisting of 90% polypropylene and 10% polyethylene. The porosity was estimated as 80% (12), and the thickness was measured as 140 μm. The liquid membranes were prepared in advance by dissolving the extractant, Acorga P5100 (Zeneca Pty Ltd), in a solvent consisting of varying quantities of *n*-decane (>99% pure, Sigma-Aldrich), Hyvis 3 (BP Chemicals, polybutene, MW = 620), Napvis XD35 (BP Chemicals, polybutene, MW = 300), and PIB (Exxon Vistanex 140 – MML polyisobutylene, MW = 2,100,000). Acorga P5100 is made from a salicyladoxime and 4-nonyl phenol, with a small amount of added kerosene. The compositions of the membranes were made on a weight basis and are given in Table 1.

Experimental Methods

During each experiment the absorbance of the strip solution, at 809 nm, was continuously monitored which enabled determination of the initial copper flux through the SLM. After the initial time of monitoring, samples of approximately 3 mL were removed periodically from both the feed and strip solutions and analyzed using the spectrophotometer to determine the copper and tartrazine concentrations. Also, the pHs of both the feed and strip solutions were

TABLE 1
Composition of Membrane Fluids (w/w%)

Fluid	P5100	*n*-Decane	Napvis 35	Hyvis 3	PIB
A	20.00	80.00	—	—	—
B	20.07	65.91	14.06	—	0.025
C	20.00	35.05	44.95	—	—
D	20.00	79.50	—	—	0.50
E	20.00	—	75.76	4.24	—
F	20.00	40.03	39.94	—	0.025
G	20.00	—	79.96	—	0.044
H	20.00	—	77.95	2.02	0.025

measured so the driving force, the pH difference, could be monitored. The lifetime of the supported liquid membrane was defined as the time between the start of the experiment and the time when tartrazine was first detected in the strip solution. After the initial time of monitoring the transfer of copper, the wavelength was changed to 425 nm and absorbance of the strip solution was monitored until tartrazine was detected.

Interfacial tensions, given in Table 3, were measured using digital imaging of the pendant drop profiles technique (4). At least three drops were averaged to determine the interfacial tension and the 95% confidence intervals for the repeat experiments.

Steady shear viscosity was measured using a Carri-med CSL100 constant stress rheometer, used in the steady rotational mode with a cone and plate geometry. Extensional viscosity measurements were determined using a Rheometrics RFX opposing jet apparatus using the 3, 2, 1, and 0.5 mm diameter nozzles. A correction to allow for inertia was required for fluids A, B, C, and F due to their low viscosities. The experimental and correction methods are described in detail elsewhere (5). Both measurements were made at 25°C.

RESULTS

SLM performance was determined for seven organic membrane liquids. Each experiment was repeated four times, except for fluids E and G, which were only repeated twice due to the long membrane life. The errors quoted are 95% confidence intervals for the repeat experiments.

It is apparent from Fig. 3 that the membrane liquid viscosity, μ, has a large effect on the rate of mass transfer through the SLM, which is expected due to the mass transfer being diffusion limited (6–8). The slope of the line of best fit through both the Newtonian and non-Newtonian data is -0.84, which leads to Eq. (1), as the flux is proportional to the diffusion coefficient, D, through the membrane.

$$D \propto \mu^{-0.84} \qquad (r^2 = 0.918) \tag{1}$$

Following the same analysis, Fig. 4 indicates that the lifetime, L, increases with membrane liquid viscosity to the power of 0.64, which leads to Eq. (2):

$$L \propto \mu^{0.64} \qquad (r^2 = 0.851) \tag{2}$$

From the regression coefficient, r^2, for each curve, it is apparent that there is greater variability associated with the life of the membrane than the initial flux. This is probably due to a greater number of variables, which may affect the membrane life compared to the flux.

There were no differences in either the initial flux or the membrane life for fluids which had polymer added, compared to those which had not. This

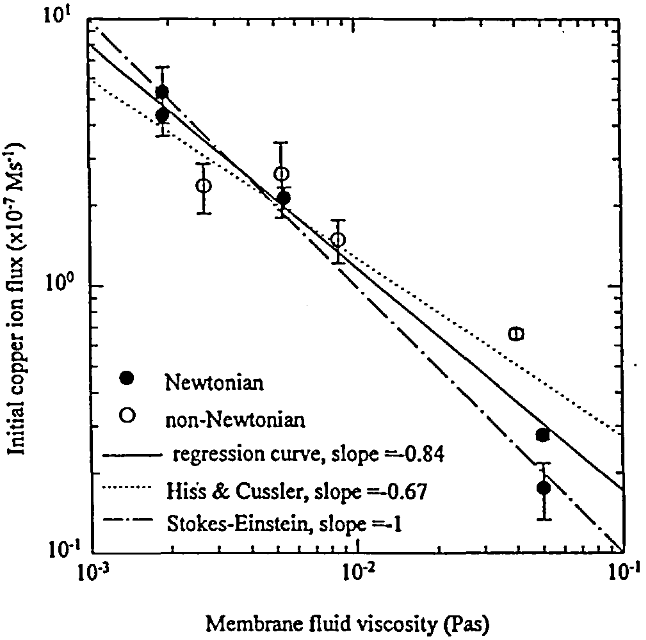

FIG. 3 Effect of rheology on initial copper flux through a supported liquid membrane.

is due to the fluids not exhibiting any elastic characteristics at the low shear rates to which they were exposed, which is discussed below.

It can be seen from Table 2 that the stirring speed has a detrimental effect on the membrane life. The detrimental effect is due to an increase in the shear force across the membrane as the stirring speed is increased.

Steady shear viscosity data for all membrane fluids are given in Fig. 5(a). All fluids exhibit constant viscosity over the shear rate range investigated. The slight scatter in the data at high and low shear rates is due to instrument limitations. The Trouton ratio, Tr, may be used as a measure of fluid elasticity. It is equal to the elongational viscosity divided by the steady shear viscosity. A Newtonian fluid will have a constant Trouton ratio equal to 3, regardless of strain rate, whereas for an elastic fluid, the Trouton ratio will increase with strain rate, and may reach a plateau. The higher the Trouton ratio, the more elastic the fluid. Figure 5(b) indicates that membrane fluids which contain polymer do exhibit elastic properties at high strain rates, and that the ones without polymer are Newtonian, as expected. Scatter in the data is due to the use of nozzles of different diameters.

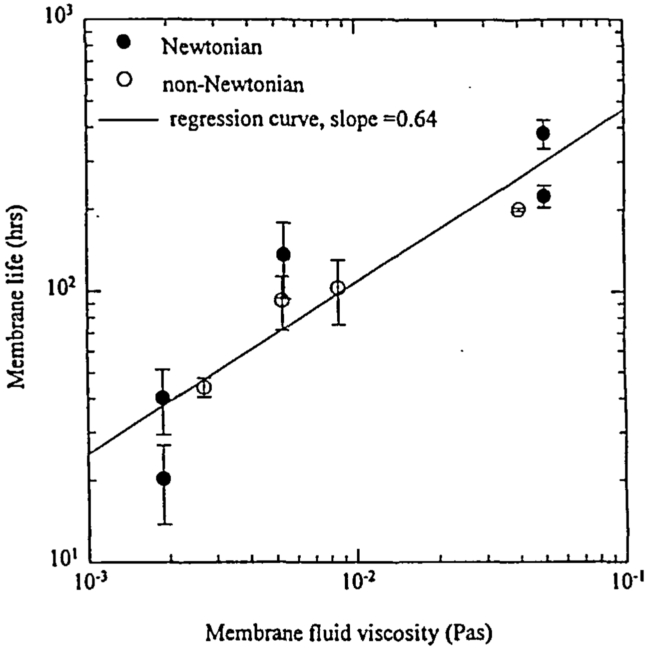

FIG. 4 Effect of rheology on supported liquid membrane life.

Table 3 indicates that the initial interfacial tension between the aqueous phase and any of the membrane liquids is quite low. It is approximately the same for either the feed or the strip solutions, and does not alter significantly with the addition of polymer. The interfacial tension at the end of an experiment was estimated by measuring the interfacial tension between membrane Fluid A, which had been saturated with feed solution, and the feed or the

TABLE 2
Effect of Stirring Speed on Supported Liquid Membrane Performance

Fluid	Stirring speed (rpm)	Initial copper flux ($\times 10^{-7}$ Ms^{-1})	SLM life (h)
A	400	4.38	52
A	600	5.31	40
A	1000	5.17	24
A	1300	5.46	22

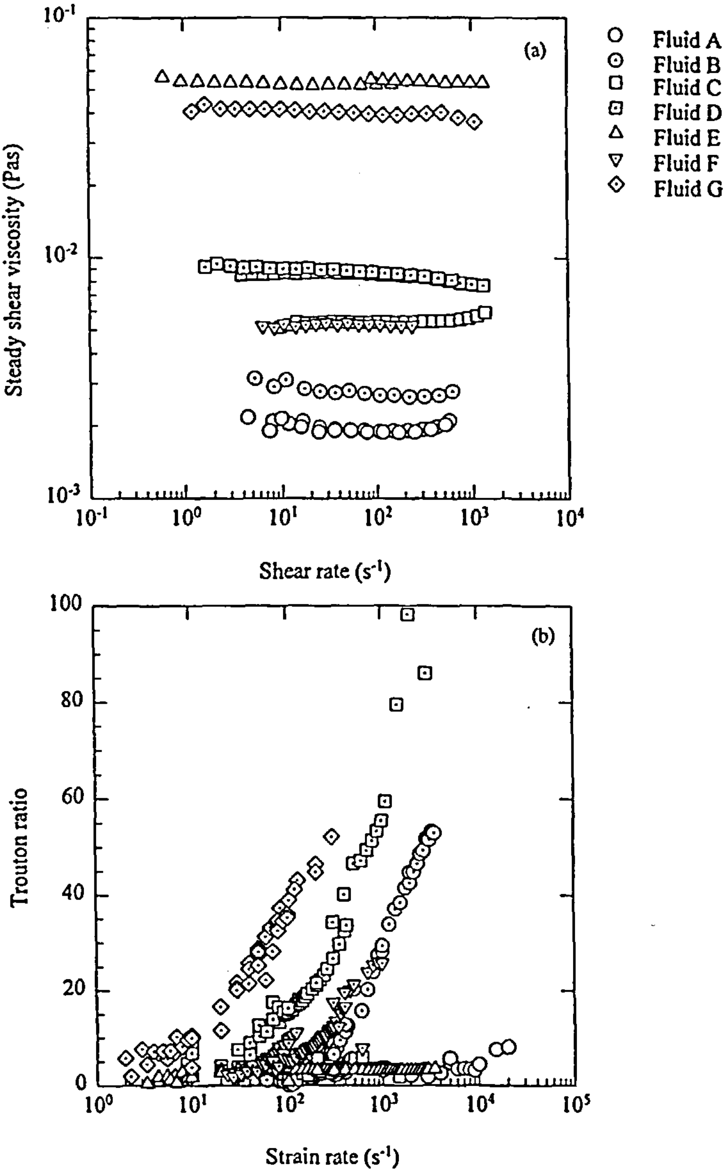

FIG. 5 (a) Steady shear viscosity and (b) Trouton ratio measurements for all membrane fluids.

TABLE 3
Initial Interfacial Tension between Aqueous Solutions and Membrane Fluids

Fluid	Initial γ-feed/membrane ($mN \cdot m^{-1}$)	Error ($\pm$%)	Initial γ-strip/membrane ($mN \cdot m^{-1}$)	Error ($\pm$%)
A	16.61	0.5	16.53	1.2
B	16.30	0.3	16.54	0.7
C	16.29	0.5	16.18	1.7
D	16.37	2.3	17.44	4.2
E	15.63	0.6	17.89	1.2
F	16.80	1.9	15.24	6.4
G	15.71	21.0	12.63	1.8

strip solutions. The interfacial tensions for the feed and the strip solutions were 18.32 and 21.14 $mN \cdot m^{-1}$, respectively. In comparison, the initial interfacial tensions were 16.61 and 16.53 $mN \cdot m^{-1}$ respectively, as given in Table 3. These results indicate that the interfacial tension does not vary significantly during the course of an experiment.

Mass transfer may cause turbulence at an interface, which is often termed the Marangoni effect. During interfacial tension measurements, drops of feed solution were observed to ''kick'' slightly when brought into contact with a membrane solution. This did not occur with the strip solution. This phenomenon was investigated further by adding talc to the aqueous phase in an attempt to visualize the interfacial turbulence using digital imaging. The feed and then the strip solutions were contacted with membrane Fluid A, both in their normal state and after saturation with the feed solution. For the saturated membrane in the feed and the strip solutions, and for the strip drops in the unaltered membrane, the only discernible movement of the talc was vertically downward due to gravity. In contrast, for feed drops in the membrane fluid, not only vertical movement but significant swirling on the drop surface was clearly visible. This continued well after the initial formation of the drop and can therefore not be attributed to circulation induced during drop formation. Also, observations of the drops of strip solution indicate that the induced circulation dissipates quickly. The swirling observed on the drop surface indicates that interfacial turbulence is present. That mass transfer has a destabilizing effect on the membrane is confirmed by comparing the SLM life in the presence and absence of mass transfer. Using Fluid A, SLM life was 40 and 110 hours in the presence and absence of the transport of copper ions, respectively.

DISCUSSION

Copper Permeability

Modeling of SLMs has been mainly limited to the mass transfer of material through the membrane. Many authors have been able to successfully model the flux through the membrane, usually based on Fick's diffusion law. Viscosity is allowed for by estimating diffusivity using the Wilke–Chang correlation (9). As the viscosity of the membrane liquid is increased, the diffusion coefficient of any species will decrease, and the rate of diffusion through the membrane and the diffusional time lag will both decrease in proportion to the diffusion coefficient.

For this system it has been established that the mass transfer is controlled by the rate of diffusion of the copper complex through the membrane (10). Although initially the rate of stripping will be slow because the concentration of the copper complex at the strip interface will be small. As mass transfer through the membrane proceeds, the complex concentration will increase and the stripping reaction will proceed at a faster rate. Therefore, initially both diffusion of the complex through the membrane and the stripping reaction may control mass transfer, but over time the stripping reaction rate will increase, leaving mass transfer controlled purely by membrane diffusion. Hughes et al. (11) also found that there was a gradual change in mechanism as the phases approached equilibrium, so that diffusional resistances became more important than chemical reaction.

The diffusion coefficient of a large solute in a solvent of small molecules follows the Stokes–Einstein equation, being inversely proportional to the fluid viscosity (12). Hiss and Cussler (13) investigated the other limiting case, of a small solute molecule diffusing in a solvent of relatively large molecules. They measured the diffusion coefficient of hexane in hydrocarbon oils of varying viscosity and found that in the viscosity range 5×10^{-3} to 5 Pa·s, the diffusion coefficient was proportional to the viscosity to the power of $-2/3$, and -1 for a viscosity below 10^{-3} Pa·s.

In this work the initial flux was found to vary with membrane liquid viscosity to the power of -0.84 for the viscosity range 2×10^{-3} to 5×10^{-2}Pa·s, as shown in Fig. 3. Deviation from the theoretical results is expected because the theories are developed for diffusion through a continuous fluid whereas diffusion will be hindered due to the membrane support in the case of an SLM. Deblay et al. (14) found that on average, the membrane support reduced diffusivity by a factor of the porosity divided by the tortuosity of the porous membrane support. The data appear to fit both theories satisfactorily as 95% confidence intervals for the regression curve encompass both the Stokes–Einstein equation and the Hiss and Cusslerz theory. Due to the experimental scatter, no conclusion may be drawn as to which is more accurate. Data taken over a wider viscosity range would help to clarify this.

Stability

Modeling of SLM stability has been restricted to equations describing the capillary pressure, from which only qualitative results are obtainable. Apart from these qualitative results, very little work has been done on the effect of viscosity, and none on the effect of elasticity on SLM performance. Danesi et al. (15) and Deblay et al. (7) considered the positive effect viscosity has on membrane stability, but neither attempted to fit a model to their data. In this work the membrane life was found to be proportional to the viscosity to the power of 0.64 for the viscosity range of 2×10^{-3} to 5×10^{-2} Pa·s, as shown in Fig. 4.

Membrane failure may be due to many factors, but a number of instability mechanisms proposed by others appear to be unlikely to have a significant effect on the system used here. The reasons are discussed below.

Solubility Effects

The Cu(II)–LIX complex exhibits very low solubility in water (16), and it is assumed that the Cu(II)–P1 complex behaves similarly. Uncomplexed P1 has a solubility in water of less than 1.8×10^{-6} M in the pH range encountered (17). *n*-Decane is insoluble in water and nonvolatile at ambient temperatures (18). The polybutenes used are strongly hydrophobic and, at ambient temperature, water solubility does not exceed 100 ppm (19). They also exhibit low volatility with no loss below temperatures of 50°C (20). Therefore, solubility of the organic into the aqueous phase is unlikely to cause membrane instability in this system.

Progressive Wetting

Progressive wetting is also unlikely to be a cause of instability in this system because the interfacial tension between the aqueous and organic phase does not change significantly during the experiment. As previously mentioned, the interfacial tension on both sides of the membrane was found to increase slightly with time, although the effect was small.

The interfacial tension increases with copper loading in the organic phase due to the low surface activity of the copper complex in comparison with the extractant (21). An increase in copper concentration in the aqueous phase will also lead to an increase in the interfacial tension since the copper will complex with the extractant at the membrane interface. Therefore, the interfacial tension on the feed side of the membrane will increase with time, although the effect may be small due to the decrease in bulk copper concentration. The reverse should be true at the strip interface, although a high concentration of sulfuric acid will diminish any increase in interfacial tension with copper concentration. Even so, the increase in interfacial tension at the strip interface is likely to be due to the increase in copper concentration in the strip solution.

Takeuchi (22) and Zha (3) both measured the advancing contact angle for an aqueous solution on a porous membrane which was immersed in the organic phase. They both found that the contact angle did not change significantly with time, although Zha found that the critical displacement pressure decreased with subsequent usage, suggesting that the contact angle may also follow the same trend. It was assumed for this work that the advancing contact angle also did not change significantly over time. If surfactants are present, as in many industrial situations, this mechanism may be important, but in these experiments it is unlikely to be significant.

Osmotic Pressure Gradient

Neplenbroek et al. (2, 23) and Zha (3) both found that an increase in the ionic strength difference between the feed and the strip solutions, leads to an increase in membrane stability. As the ionic strength increased, the osmotic pressure exerted on the membrane also increased. If the osmotic pressure gradient was the cause of instability, an increase in osmotic pressure would lead to decreased stability, which is clearly not the case. In light of their work it is doubtful that the osmotic pressure gradient is the cause of initial membrane instability. Instead, they found that emulsification of the organic was the major cause of membrane liquid loss.

Hydrodynamic Instability

Shearing forces across a membrane can lead to instabilities at the fluid interface, resulting in membrane instability (2, 3). Capillary ripples and the Tollmien–Schlichting and the Kelvin–Helmholtz instabilities are fundamentally associated with fluids that are in motion, whereas the Rayleigh–Taylor and the Benard instabilities can occur in fluids at rest (24). For films that have moderate motion the Rayleigh–Taylor and the Benard instabilities will be less significant than the other instabilities because the body forces will be small relative to the inertia forces (24). The Kelvin–Helmholtz instability is also likely to occur before the Tollmien–Schlichting instability because the former has been found to occur even if the two fluids are in laminar motion. For the case of a supported liquid membrane the aqueous fluids are always under forced flow across the membrane, whether it be by stirring or pumping. Therefore, it is to be expected that capillary ripples and the Kelvin–Helmholtz instability will have an important bearing on the stability of the aqueous–

organic fluid interface. The Benard instability is not likely to have a great influence on stability as in this case the gravitational force acts parallel to the interface.

The Kelvin–Helmholtz instability arises when two liquids move with different tangential velocities across an interface. For the case of two uniform liquids with constant interfacial tension in relative horizontal motion separated by a horizontal boundary, any perturbation will be suppressed if (25)

$$p < \frac{g(\rho_1^2 - \rho_2^2)}{\rho_1 \rho_2 (u_1 - u_2)^2} \tag{3}$$

where p is the wavenumber, g the acceleration due to gravity, u the fluid velocity, and the subscripts 1 and 2 denote the lower, or more dense fluid, and upper fluid, respectively. Also, the interfacial tension will suppress the Kelvin–Helmholtz instability if (25)

$$(u_1 - u_2)^2 < 2(\rho_1 + \rho_2) \frac{[g\gamma(\rho_1 - \rho_2)]^{1/2}}{\rho_1 \rho_2} \tag{4}$$

For this membrane system, Eq. (4) suggests that the organic/aqueous interface will be stable if the velocity difference between the two phases is less than 0.16 m·s^{-1}. A velocity difference in this order is expected to be obtained in the aqueous phase, considering the tip velocity of the stirrer moved at approximately 0.8 m·s^{-1}. The shear rate at the membrane face, S, was calculated to be approximately 10 s^{-1} using Eq. (5) (26), where f is the stirring rate in revolutions per second, and a and b are the radii of the stirrer and chamber, respectively:

$$S = \frac{4\pi f a^2}{b^2 - a^2} \tag{5}$$

From Eq. (3), a wavenumber of 353 m^{-1} corresponded to a velocity difference of 0.16 m·s^{-1} and, therefore, the maximum wavelength at which suppression of the disturbance occurs is 1.8 cm.

Zha (3) showed that the rate of membrane liquid loss was initially high and then decreased. This indicates that there are two regions of membrane liquid loss, that from the surface film, which is quickly removed, and that from the support pores. The loss from the surface is likely to be due to hydrodynamic instabilities, in particular the Kelvin–Helmholtz instability, causing the membrane liquid to break up into drops. This is due to the fact that the stirring speed has a large effect on the membrane life, and that with a 6-cm^2 membrane, a wavelength of greater than 1.8 cm could possibly be sustained. Once the surface excess has been removed, the membrane liquid resides in the pores of the support. The pore size of membrane supports is usually less than 1 µm, 0.45 µm in this case, making it only possible for wavelengths much lower than that required for instability to exist. Therefore, hydrodynamic instabilities appear unlikely to be the cause of further membrane liquid loss. An increase in fluid viscosity will decrease the Kelvin–Helmholtz instability, mainly due to enhanced damping (27, 29), but interfacial tension gradients may increase it (28).

Marangoni Effect

Although the overall interfacial tension does not appear to be the cause of instability, local changes in interfacial tension at the organic/aqueous interface due to mass transfer will lead to interfacial disturbances. Zha (3) found that Marangoni effects could lead to membrane instability for some systems, but discounted it for the copper system due to no observed "kicking" of a drop formed at a glass tip. "Kicking," or erratic pulsations of a drop, are caused by local changes in interfacial tension, resulting in local interfacial tension gradients. The Marangoni effect may be present and no "kicking" observed if the disturbance is not great enough. The Marangoni effect is explained in detail by Sternling and Scriven (29), who also found that viscosity will decrease the effect, because surface waves will be damped. They also give examples of systems where spontaneous interfacial activity and, in some cases, emulsification will occur at flat or rounded interfaces.

The observation of drops of the aqueous solutions immersed in the membrane phase clearly indicate that interfacial turbulence is present at the feed side of the membrane and is caused by mass transfer. The fact that it does not occur at the strip interface could be due to a slower reaction occurring there. Neplenbroek et al. (2) also found that instability was greater at the feed interface.

Local interfacial tension gradients at the membrane interface may be caused by mass transfer or induced by shear. Surface waves, which are enhanced by shear forces across the interface, will be set up within the pores. When the disturbance is large enough, small drops will break away from the interface and be entrained in the bulk fluid. The rate of stirring has a negative impact on membrane stability (2, 3, 30), as also shown in Table 2. This is due to an increase in the shear force at the membrane, which will enhance any instabilities already present. Increasing the shear across the membrane will increase the occurrence of concentration gradients, and therefore interfacial tension gradients, and will also cause drops of the membrane liquid to be more easily entrained in the flow of the bulk fluid.

Effect of Rheology

Figures 3 and 4 show that the flux through the membrane and the life of the membrane are only dependant on the membrane liquid viscosity and not on the addition of polymer. The trends observed for purely viscous fluids were expected, but the result that polymer addition has no effect was quite unexpected. An elastic fluid resists flow to a greater extent than a purely viscous one, so it will exhibit greater resistance to the forces pulling it from the membrane pores and thus exhibit a longer life. This clearly does not occur in these experiments.

Figure 3 indicates that the flux through the membrane decreased with viscosity, but showed no change due to the addition of polymer. No clear trend has been established for the effect of polymer addition on diffusion rates in either aqueous or organic liquids. Both increases and decreases in the diffusion rate have been observed in various systems (31–33). Little work has been conducted with organic solutions, but both Jones and Gainer (32), and Wright (31) found that the diffusion rate decreased in their organic solutions. A few authors have proposed reasons for the change in the diffusion rate due to the presence of polymer. Metzner (33) attributed an increase in diffusion rates to the polymer creating a structured media through the solvent, and Ponter and Davies (34) concluded that polymeric molecules have little effect on molecular transport of solute but have a profound effect on the flow properties of the solution. In this work no effect on the flux through the membrane was observed for the non-Newtonian fluids. This may be due to the large errors associated with the measurements overshadowing any difference in the flux as variations would have to be large to be distinguished from experimental scatter. Variations in the porous membrane support also contribute to the high level of experimental error.

As illustrated in Fig. 4, the membrane life, as expected, increased with viscosity. An increase in viscosity will damp surface waves, inhibiting any interfacial disturbance. A more viscous fluid is also less likely to break into drops. Neplenbroek et al. (35) achieved the same effect by applying a thin dense gel layer to the feed side of the membrane.

As shown above, the shear rate at the membrane surface was estimated to be in the order of 10 s^{-1}. Figure 5(b) indicates that at such low shear rates the membrane fluids exhibited no elastic properties, and all behaved as Newtonian fluids. Therefore, no difference in the SLM life was observed for membrane fluids, with or without the addition of polymer, as long as the viscosity was constant. In a system where the shear rates across the membrane were at least an order of magnitude higher, an enhancement of the life with polymer addition would be expected. This enhancement is due to the fact that an elastic fluid exhibits greater resistance to motion than a purely viscous one. Therefore, surface waves would be damped to a greater extent and the membrane liquid would be less likely to break into drops.

Optimum Performance

Increasing membrane liquid viscosity will improve the stability of an SLM, but it will also have a detrimental effect on mass transfer. To optimize the

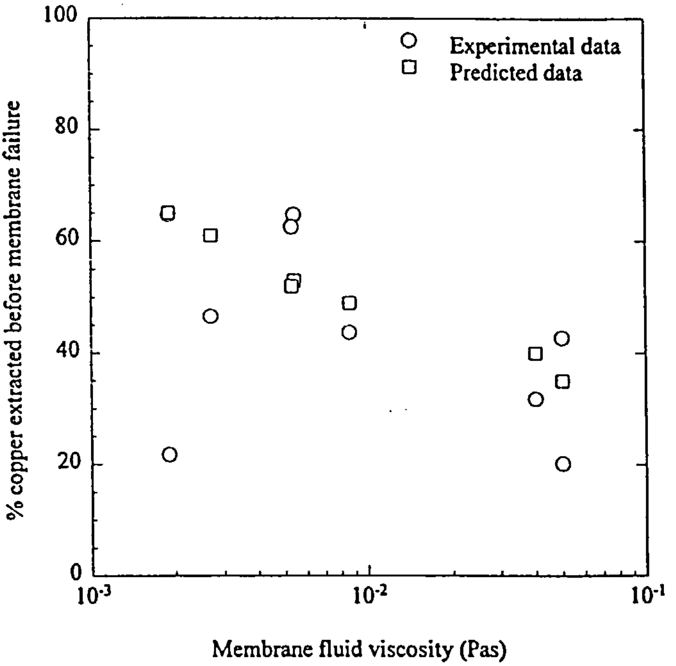

FIG.6 Percentage of copper extracted before membrane failure versus membrane fluid viscosity.

performance of an SLM, a balance between the stability and the rate of mass transfer must be achieved. Figure 6 indicates that for the type of SLMs used in this work, the improved stability achieved by increasing the membrane viscosity is counteracted by the decrease in the mass transfer. These results were achieved in a batch system where the driving force was left to decline naturally. If the driving force was kept constant, the flux would also remain constant and not decline with time. Figure 6 illustrates that if this were the case, the same trend would be observed. Therefore, for these SLMs in the viscosity range of 2×10^{-3} to 5×10^{-2} Pa·s, highest extraction was achieved at the lowest viscosity.

It should be noted that only one type of membrane support was investigated, and that a different conclusion may be reached using a different membrane. For example, increased stability may be achieved using a membrane with smaller pores (22) without any decrease in flux, so long as the membrane porosity and tortuosity remain constant (7).

CONCLUSION

For the SLM investigated it was found that an increase in membrane fluid viscosity decreased the copper flux but improved the membrane stability. In the viscosity range of 2×10^{-3} to 5×10^{-2} Pa·s, optimum performance was achieved using a membrane fluid of the lowest viscosity. Even though a fluid of higher viscosity had greater stability, the decrease in mass transfer outweighed the benefits of a more stable membrane.

The destabilization of the membrane was found to be due to two mechanisms, interfacial turbulence as a result of mass transfer, termed the Marangoni effect, and hydrodynamic instabilities due to stirring effects. Membrane liquid removal occurred due to the onset of instability at the interface. When the instabilities grew large enough, the membrane liquid broke into drops and was entrained in the aqueous phase. Liquid removal occurred in two stages. First, the surface excess on the membrane was removed as hydrodynamic instabilities were set up by the shearing action of the stirrer. Once all the surface excess was emulsified, the remaining membrane liquid resided in the pores, the diameter of which are too small for hydrodynamic instabilities to occur. Instability then occurred due to the Marangoni effect, primarily at the feed interface. Shear forces across the membrane face, caused by stirring, enhanced any disturbance. The shear forces also aided in the expulsion of the organic from the membrane support in small drops, and the consequent entrainment of the drops in the continuous fluid.

The addition of polymer had no effect on the initial flux through the membrane, nor on the membrane stability. The initial flux for the Newtonian and non-Newtonian results were the same, given the large experimental error. Polymer addition had no effect on membrane stability due to the low shear rates encountered at the membrane surface. At low shear rates none of the membrane fluids exhibited any significant degree of elasticity, and therefore behaved as purely Newtonian fluids.

NOMENCLATURE

a	radius of stirrer (m)
b	radius of chamber (m)
D	diffusion coefficient ($m^2 \cdot s^{-1}$)
f	stirring rate (Hz)
g	acceleration due to gravity ($m \cdot s^2$)
L	membrane life (h)
p	wavenumber (—)
r^2	regression coefficient (—)
S	shear rate at membrane interface (s^{-1})

Tr	Trouton ratio (—)
u	velocity ($m \cdot s^{-1}$)

Greek

γ	interfacial tension ($N \cdot m^{-1}$)
κ	conductivity ($S \cdot cm^{-1}$)
μ	viscosity ($Pa \cdot s$)
ρ	density ($kg \cdot m^{-3}$)

Subscripts

1	lower (more dense) fluid
2	upper fluid

ACKNOWLEDGMENTS

This work was funded by City West Water Ltd., the Advanced Mineral Products Centre, and the Australian Research Council. The GORE-TEX laminate was kindly supplied by W. L. Gore and Associates (Aust.) Pty. Ltd, Acorga P5100 by Zeneca Pty. Ltd., and the polybutene fluids by BP Chemicals Ltd.

REFERENCES

1. P. Danesi, *Sep. Sci. Technol.*, *19*(11&12), 857–894 (1984–5).
2. A. Neplenbroek, D. Bargeman, and C. Smolders, *J. Membr. Sci.*, *67*, 133–148 (1992).
3. F-F. Zha, Ph.D. Thesis, University of New South Wales, Sydney, 1993.
4. P. Lyford, Ph.D. Thesis, University of Melbourne, 1996.
5. C. G. Hermansky and D. V. Boger, *J. Non-Newtonian Fluid Mech.*, *56*, 1–14 (1995).
6. R. W. Baker, M. E. Tuttle, D. J. Kelly, and H. K. Lonsdale, *J. Membr. Sci.*, *2*, 213–233 (1977).
7. P. Deblay, S. Delepine, M. Minier, and H. Renon, *Sep. Sci. Technol.*, *26*(1), 97–116 (1991).
8. A. A. Elhassadi and D. D. Do, *Ibid.*, *21*(3), 267–283 (1986).
9. C. R. Wilke and P. Chang, *AIChE J.*, *1*, 264–270 (1955).
10. T. M. Dreher, *Ph.D. Thesis*, University of Melbourne, 1996.
11. M. A. Hughes, J. S. Preston, and R. J. Whewell, *J. Inorg. Nucl. Chem.*, *38*, 2067–2069 (1976).
12. S. Claesson, W. Kern, P. H. Norberg, and W. Heitz, *Makromol. Chem.*, *87*, 1–7 (1965).
13. T. G. Hiss and E. L. Cussler, *AIChE J.*, *19*, 698–703 (1973).
14. P. Deblay, M. Minier, and H. Renon, *Biotechnol. Bioeng.*, *35*, 123–131 (1990).
15. P. R. Danesi, L. Reichley-Yinger, and P. G. Rickert, *J. Membr. Sci.*, *31*, 117–145 (1987).
16. A. W. Ashbrook, *Anal. Chim. Acta*, *58*, 115–121 (1972).
17. H. J. Foakes, J. S. Preston, and R. J. Whewell, *Ibid.*, *97*, 349–356 (1978).

18. R. C. Weast and M. J. Astle (Eds.), *CRC Handbook of Data on Organic Compounds, Vol. 1*, CRC Press, Florida, 1985, p. 537.
19. BP Chemicals Technigram, *Polybutenes Literature* (PB 902), BP Chemicals Ltd., London, 1990.
20. BP Chemicals Technigram, *Polybutenes Literature* (PB 108), BP Chemicals Ltd., London, 1989.
21. K. Takahashi, and H. Takeuchi, *J. Chem. Eng. Jpn.*, *19*, 161–166 (1986).
22. H. Takeuchi, *Mem. Fac. Eng., Nagoya Univ.*, *43*(1) (1991)
23. A. Neplenbroek, D. Bargeman, and C. Smolders, *J. Membr. Sci.*, *67*, 121–132 (1992).
24. S. Ostrach and A. Koestel, *AIChE J.*, *11*(2), 294–303 (1965).
25. S. Chandrasekhar, *Hydrodynamic and Hydromagnetic Stability*, Oxford University Press, Oxford, 1961.
26. T. J. Pedley, *Q. Rev. Biophys.*, *16*, 115–150 (1983).
27. E. S. R. Gopal, in *Emulsion Science* (P., Sherman, Ed.), Academic Press, London, 1968 Chap. 1.
28. P. Walstra, in *Encyclopedia of Emulsion Technology, Vol. 1* (P. Becher, Ed.), Dekker, New York, NY, 1983 Chap. 2.
29. C. V. Sternling and L. E. Scriven, *AIChE J.*, *5*, 514–523 (1959).
30. H. Takeuchi, K. Takahashi, and W. Goto, *J. Membr. Sci.*, *34*, 19–31 (1987).
31. J. E. Wright, Ph.D. Thesis, The University of Melbourne, 1994.
32. R. C. Jones and J. L. Gainer, *Ind. Eng. Chem. Fundam.*, *15*, 83–85 (1976).
33. A. B. Metzner, *Nature*, *208*, 267–268 (1965).
34. A. B. Ponter and G. A. Davies, *Nature*, *210*, 837 (1966).
35. A. Neplenbroek, D. Bargeman, and C. Smolders, *J. Membr. Sci.*, *67*, 149–165 (1992).

Received by editor May 2, 1997
Revision received August 1997